2005 American Control Conference
June 8-10, 2005. Portland, OR, USA

An Adaptive Inverse Control Scheme for A Synthetic Jet Actuator Model

Dipankar Deb, Gang Tao, Jason O. Burkholder and Douglas R. Smith

Abstract— **In this paper, we develop an adaptive inverse compensation scheme for controlling the aerodynamic flow of a synthetic jet actuator on a dynamic aircraft system. An adaptive inverse is employed for cancelling the effect of the nonlinearity of the synthetic jet. A linear state feedback control law is used for controlling the aircraft dynamics. A linearly parametrized error model is derived for the nonlinear actuator model. A parameter projection adaptive law is used to ensure desired closed-loop stability and asymptotic tracking. An application of this adaptive compensation scheme to the control of a linear aircraft model with a synthetic jet actuator is studied and its effectiveness is verified by simulation results.**

Keywords: Actuator nonlinearity, adaptive inverse, parameter projection, stability and tracking, synthetic jets.

I. Introduction

Interest in active flow control for drag or noise reduction, flow vectoring, mixing enhancement, and separation control has stimulated recent development in the area of synthetic jet actuators. The zero-net-mass nature of a synthetic jet actuator makes it an attractive boundary layer flow controller. Advantages of using it are low cost, compact structure and ease of operation. Typically, the flow over a wing is smooth and steady with streamlines parallel to the surface. When a flow separates, the flow next to the surface is no longer smooth and steady, and the turbulent flow that results is far more vigourous than turbulence in a turbulent boundary layer. At the point of separation, where the fluid velocity is zero, a streamline originates at the surface and moves away. The flow downstream of this point is the separated flow, and in general is moving opposite to the flow upstream. Should the flow near the surface again become smooth and steady after separation, then it is called reattached flow. The synthetic jets will be actuated to cause the turbulent boundary layer to reattach and the control signal modulated to control the shape of the downstream reattachment.

Flow control studies have shown that synthetic jet actuators are efficient devices for controlling separated flows [2], [12]. Smith et al. [12] and Amitay et al. [1] have used synthetic jet control on an airfoil to prevent boundary layer separation at high angles of attack. Large gains in lift and dramatic reductions in drag were realized. Using a circular cylinder model, Honohan et al. [7] showed that synthetic jet actuators can, in the mean, displace flow streamlines and create apparent closed flow regions adjacent to a surface and downstream of the actuator. A consequence of creating these recirculation zones is that the acceleration of the flow around the interaction region leads to local changes in the surface pressure distribution. In order to create a similar effect on an airfoil, Amitay et al. [3] used a synthetic jet actuator in conjunction with a small surface obstacle that caused separation. This configuration allows synthetic jets to control the degree of flow separation and consequently airfoil shape change. The interaction of the jets with a cross flow results in an apparent modification of the surface shape and is exploited for dynamic control of flow reattachment and separation over a thick airfoil.

In [6], numerical simulations have been provided on microfabricated arrays of synthetic jets for enhanced aerodynamic flow performance. In [5], scaling and operational characteristics of a synthetic jet is provided. Feedback control applications require the actuator transfer function that relates the input voltage to the output position control of the dynamic system. In [1], synthetic jet actuators are investigated on a symmetric airfoil under different wind tunnel testing conditions. It studies pressure distribution on the airfoil at different angles of attack and at different angles (i.e., azimuthal angles) of actuation. The results also give an improved understanding of effect of reattached flow on the strength of control input.

When used in conjunction with a separation-inducing device at low angles of attack, synthetic jets can create a new virtual shape of the airfoil so as to reduce drag and/or to increase lift under normal flight conditions. In this paper, a preliminary theoretical model for this application is presented. In order to achieve desired system performance, we use an adaptive control design so as to provide desired adaptation to adjust a controller for parametric uncertainty. Adaptive control algorithms based on an adaptive inverse approach have been formulated by Tao et al. [13] and [14].

In this paper, we developed such an adaptive control system to meet a desired control objective with a synthetic jet actuator. The paper is organized as follows. In Section 2, we provide a physical description and mathematical modeling of the synthetic jet actuator. In Section 3, we propose and analyze an adaptive inverse compensation model so as to

Dipankar Deb and Gang Tao are with Charles L. Brown Department of Electrical and Computer Engineering, University of Virginia, Charlottesville, VA, 22904, (email: dd8v, gt9s@virginia.edu)

Jason O. Burkholder is with Barron Associates, Inc., 1410 Sachem Place, Suite 202, Charlottesville, VA 22901 (email: burkholder@bainet.com)

Douglas R. Smith is with Department of Mechanical Engineering, University of Wyoming, Laramie, WY 82071 (email: drsmith@uwyo.edu)

This research was partially supported by the U.S. Air Force under an STTR contract.

cancel the effect of the unknown actuator nonlinearity. We also present some inverse related issues and the control error caused by parametric uncertainty. In Section 4, we present a state feedback control law. In Section 5, we design and analyze a parameter projection based adaptive law. In Section 6, simulation results verify the desired system. We also study the effect of saturation through simulation results.

II. Synthetic Jets for Aircraft Control

In this section, we first give a physical description of a synthetic jet actuator and explain how it alters the virtual shape of an airfoil, and then present a mathematical model of the actuator nonlinearity. The schematic structure of a synthetic jet actuator is shown in Figure 1.

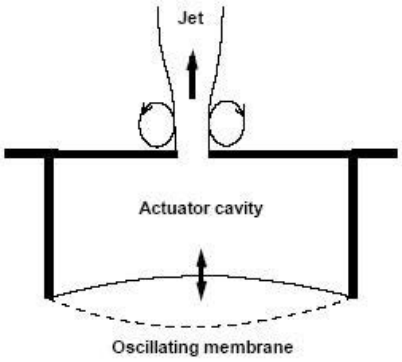

Fig. 1. Synthetic jet actuator [9].

A. Physical Description

A synthetic jet actuator is a zero-net mass flux device that produces non-zero fluid momentum across an orifice. The jet is synthesized by a train of vortices formed at the edge of the orifice by an oscillating membrane driven at its resonating frequency. The motion of the diaphragm is induced by a piezo-electric device, which causes pressure fluctuations inside the cavity. These pressure variations force fluid in and out of the cavity via an orifice. A mean jet flow is established external to the orifice on the other side of the cavity, without the presence of a fluid source.

B. Mathematical Model

Consider a synthetic jet actuator which can be characterized by a nonlinearity $N(\cdot)$:

$$u(t) = C_l(t) = N(v(t)) = N(A_{pp}^2(t)), \tag{1}$$

where $v(t) = A_{pp}^2$ with $A_{pp}(t)$ being the input peak-to-peak voltage amplitude of the synthetic jet, and $u(t) = C_l(t)$ is the equivalent virtual deflection on the airfoil. For a general actuator nonlinearity compensation problem, we assume that

- the output $u(t)$ of the actuator nonlinearity $N(\cdot)$ is not accessible for measurement, and
- the parameters of $N(\cdot)$ are unknown.

The synthetic jet is actuated so that the control signal generated favorably changes the virtual shape of the airfoil. The jet momentum is assumed to be constant during the entire period of the diaphragm motion. Under conditions of constant airstream density and control of flow along the width, the synthetic jet block can be modeled as

$$C_l(t) = p_1 - \frac{p_2 p_3 U_\infty}{f c C_\mu(t)}, \tag{2}$$

where $C_\mu(t)$, the momentum coefficient of the actuator is

$$C_\mu(t) = \frac{p_4 A_{pp}^2(t)}{U_\infty^2}.$$

The frequency of the input voltage $v(t)$ is f, the local wing chord is c, the freestream velocity is U_∞ and unknown parameters of certain physical meaning are p_i, i = 2, 3, 4. The maximum deflection that can be achieved is p_1. The effect of the synthetic jet on lift can be translated to an effective surface deflection.

The control objective is to design an adaptive compensator to cancel the effect of an uncertain actuator nonlinearity $N(\cdot)$, to apply a feedback control law for aircraft control. We present a parametrized nonlinearity model suitable for adaptive compensation design. The actuator resonance frequency is treated as constant. We control the actuator output by controlling the peak-to-peak voltage amplitude. The parameters $p_1 = 15$, $p_2 = 0.05$, $p_3 = 0.05$ and $p_4 = 5$ are chosen arbitrarily as a baseline model. The values f = 60Hz, and c = 2ft and U_∞ = 200 ft/sec are taken as a standard. The simplified model with these parameters is

$$C_l(t) = 15 - \frac{33.33}{A_{pp}^2(t)}. \tag{3}$$

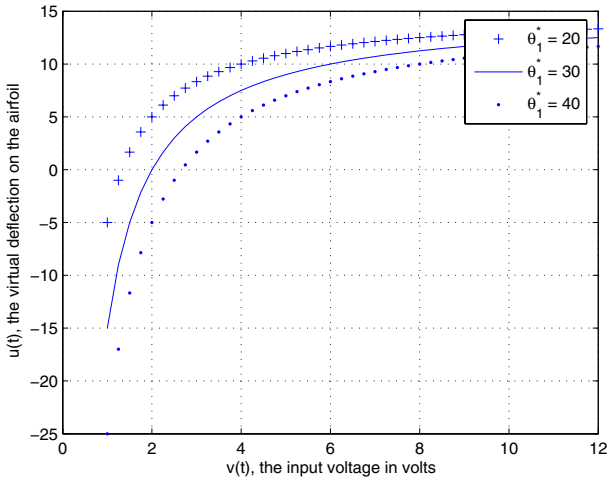

Fig. 2. Variation of virtual surface deflection with actuation voltage.

Figure 2 shows variations of deflection on the surface of the airfoil against actuator voltage magnitude at different values of parameter θ_1^*.

Nonlinearity model. In order to perform adaptive compensation, we consider a parametric model with parameters $\theta^* = [\theta_1^*, \theta_2^*]^T \in R^2$ for the nonlinearity $N(\cdot)$, given by

$$u(t) = \theta_2^* - \frac{\theta_1^*}{v(t)} = N(\theta^*; v(t)). \quad (4)$$

III. Adaptive Inverse

An adaptive inverse control design for a plant with parametrized actuator nonlinearity $N(\theta^*; v(t))$ requires a nonlinearity inverse as a compensator for the unknown nonlinearity $N(\cdot)$. We employ the adaptive inverse

$$v(t) = \widehat{NI}(u_d(t)) = \frac{\theta_1(t)}{\theta_2(t) - u_d(t)}, \quad (5)$$

where $\theta(t) = [\theta_1(t), \theta_2(t)]^T$ is an adaptive estimate of θ^*, and $u_d(t)$ is the desired control signal from a feedback law.

Inverse related issues. The inverse parameters θ are to be updated from adaptive laws and should stay in prespecified regions (that is, $\theta_1, \theta_2 > 0$, because $\theta_1^*, \theta_2^* > 0$), needed for implementation of the inverse. This will be ensured by adaptive laws based on parameter projection algorithm. We assume that the desired control signal from a state feedback law satisfies

(A1) $u_d(t) < \theta_2(t), \forall t \geq 0$,

so that the adaptive inverse is singularity-free. Assumption (A1) and parameter $\theta_1(t) > 0$ ensure that $v(t) \neq 0$ and so (2.4) is non-singular.

Control error. An expression of the control error $u(t) - u_d(t)$ is critical for designing adaptive laws. Using (4) and (5), we obtain

$$u(t) = \frac{\theta_2^* \theta_1(t) - \theta_1^*(\theta_2(t) - u_d(t))}{\theta_1(t)}. \quad (6)$$

Thus, the control error is

$$u(t) - u_d(t) = \left(\frac{\theta_2(t) - u_d(t)}{\theta_1(t)}\right)(\theta_1(t) - \theta_1^*) - (\theta_2(t) - \theta_2^*), \quad (7)$$

where $\theta_2(t) - u_d(t)$ is available and $\theta_1(t), \theta_2(t)$ are updated.

IV. Feedback Control System

We present a state feedback adaptive inverse control scheme to cancel the nonlinearity $N(\theta^*; v(t))$, in order to meet the control objective. Such a control system is

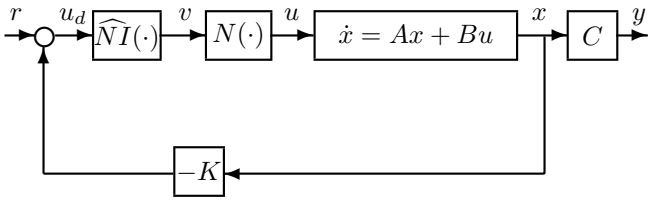

Fig. 3. State feedback inverse control.

shown in Figure 3 (note that the output y(t) is not used in this study). As a preliminary study of adaptive inverse control, we consider a linear time-invariant plant which has a controllable state variable form

$$\dot{x}(t) = Ax(t) + Bu(t),\ x(t) \in R^{n\times n},\ u(t) \in R, \quad (8)$$

where $u(t)$ is the plant input, and $A \in R^{n\times n}$ and $B \in R^{n\times 1}$ are known constant matrices. Recall that the signal $u(t)$ is the output of the actuator $N(\cdot)$, that is $u(t) = N(v)$.

The desired state feedback control signal is

$$u_d(t) = -Kx(t) + r(t), \quad (9)$$

where $r(t)$ is a bounded reference input signal and $K \in R^{1\times n}$ is a constant gain vector such that the eigenvalues of $A - BK$ are equal to some desired closed-loop system poles. The choice of such a K can be made from an LQR design [8] or a pole placement technique [11].

Using (7), (8), and (9), we get

$$\begin{aligned}\dot{x}(t) &= (A - BK)x(t) + Br(t) - B(\theta_2(t) - \theta_2^*) \\ &\quad + B\left(\frac{\theta_2(t) - u_d(t)}{\theta_1(t)}\right)(\theta_1(t) - \theta_1^*). \end{aligned} \quad (10)$$

This equation motivates us to choose the reference model

$$\dot{x}_m(t) = (A - BK)x_m(t) + Br(t). \quad (11)$$

The control objective is to choose a feedback gain K and adaptive laws for inverse parameters $\theta(t)$, such that closed-loop signals are bounded, $\lim_{t\to\infty}(x(t) - x_m(t)) = 0$.

V. Adaptive Laws

In this section, we formulate adaptive laws to update the estimates $\theta_i(t), i = 1, 2$ so that the control objective is achievable. Parameter projection is used to guarantee the boundedness of $\theta(t)$ by lower bounds so that the adaptive inverse is meaningful. We assume that the lower bounds of the true nonlinearity parameters θ_i^* are known, i.e., $\theta_i^a \leq \theta_i^*$ for some known constants $\theta_i^a > 0$, such that for $\theta_i(t) \geq \theta_i^a$, the characteristic $N(\theta_i(t); v(t))$ renders a nonlinearity model of the same type as that of the true nonlinearity model $N(\theta_i^*; v(t))$. Initial estimates $\theta_i(0)$ of θ_i^* are chosen such that $\theta_i(0) \geq \theta_i^a$.

We choose the adaptive laws for $\theta_1(t), \theta_2(t)$ as

$$\dot{\theta}_i(t) = g_i(t) + f_i(t),\ i = 1, 2,\ t \geq 0, \quad (12)$$

$$\text{where } g_1(t) = -\gamma_1 e^T(t) PB \frac{(\theta_2 - u_d(t))}{\theta_1},$$

$$g_2(t) = \gamma_2 e^T(t) PB,$$

with tracking errors $e(t) = x(t) - x_m(t)$, adaptation gains $\gamma_i > 0, i = 1, 2$ and $P \in R^{n\times n}, P = P^T > 0$ satisfying

$$PA_m + A_m^T P = -Q,\ A_m = A - BK \quad (13)$$

for a constant matrix $Q \in R^{n\times n}$ such that $Q = Q^T > 0$,

$$f_i(t) = \begin{cases} 0 & \text{if } \theta_i(t) > \theta_i^a, \text{ or} \\ & \text{if } \theta_i(t) = \theta_i^a \text{ and } g_i(t) \geq 0 \\ -g_i(t) & \text{otherwise.} \end{cases} \quad (14)$$

Theorem 1: Under assumptions (A1), the control law (9), with adaptive laws (12) and the inverse (5), applied to the plant (8), guarantees that all closed-loop signals are bounded and $\lim_{t\to\infty} e(t) = 0$.

Proof: Using (10), (11), $\tilde{\theta}_1(t) = \theta_1(t) - \theta_1^*$, $\tilde{\theta}_2(t) = \theta_2(t) - \theta_2^*$, we have

$$\dot{e}(t) = (A - BK)e(t) + B\left(\left(\frac{\theta_2(t) - u_d(t)}{\theta_1(t)}\right)\tilde{\theta}_1 - \tilde{\theta}_2\right). \tag{15}$$

Consider the positive definite function

$$V(e, \tilde{\theta}_1, \tilde{\theta}_2) = e^T P e + \tilde{\theta}_1^2 \gamma_1^{-1} + \tilde{\theta}_2^2 \gamma_2^{-1} \tag{16}$$

as a measure of the system errors $e, \tilde{\theta}_1$ and $\tilde{\theta}_2$. The time derivative of $V(e_c)$ is

$$\dot{V} = e^T(t)P\dot{e}(t) + \dot{e}^T(t)Pe(t) + 2\sum_{i=1}^{2} \tilde{\theta}_i(t)\gamma_i^{-1}\dot{\theta}_i(t). \tag{17}$$

Substituting (12) and (13) into (15), and noting that $\dot{\tilde{\theta}}_i(t) = \dot{\theta}_i(t)$, $i = 1, 2$, the time derivative of V is

$$\dot{V} = -e^T(t)Qe(t) + 2\tilde{\theta}_1(t)\gamma_1^{-1} f_1(t) + 2\tilde{\theta}_2(t)\gamma_2^{-1} f_2(t). \tag{18}$$

With $\theta_1(0) \geq \theta_1^a$, $\theta_2(0) \geq \theta_2^a$ and from the parameter projection algorithm (14), it follows that

$$\theta_i(t) \geq \theta_i^a, \;\; \tilde{\theta}_i(t) f_i(t) \leq 0, i = 1, 2.$$

With this property, (18) becomes

$$\dot{V} = -e^T(t)Qe(t) \leq 0. \tag{19}$$

From which we have, $e(t), \theta_1(t)$ are uniformly bounded and $e(t) \in L^2$. From (15), $\dot{e}(t)$ is bounded. Therefore, we conclude that $\lim_{t\to\infty} e(t) = 0$. $\bigtriangledown$

This adaptive control scheme has unique technical features hitherto unaddressed in the literature [13], [14], such as the nonlinearity parametrization (4), the nonlinearity adaptive invere (5), and the parameter dependence of $g_1(t)$ in the adaptive law (12) to cope with the nonlinearity parametrization for the inverse adaptation.

Thus far, we have developed an adaptive inverse control scheme for the synthetic jet model, under the assumption (A1): the control signal $u_d(t)$ is less than $\theta_2(t), \forall t \geq 0$. A further topic of research is to relax this assumption, which is currently being investigated. Though it is not imperative, for simulation study and demonstration of desired performance of adaptive inverse control, we assume that $\theta_2 = \theta_2^* = p_1$.

(A2) the parameter p_1 (which denotes the saturation level of the synthetic jet actuator) is known.

Under this assumption, (7) reduces to

$$u(t) - u_d(t) = \frac{(\theta_2 - u_d(t))(\theta_1(t) - \theta_1^*)}{\theta_1(t)}, \tag{20}$$

thereby reducing the state system (10) to

$$\dot{x}(t) = (A - BK)x(t) + Br(t) + B\left(\frac{\theta_2(t) - u_d(t)}{\theta_1(t)}\right)\tilde{\theta}_1(t), \tag{21}$$

where $\tilde{\theta}_1(t) = \theta_1(t) - \theta_1^*$.

With assumptions (A1): $u_d(t) < \theta_2(t), \forall t \geq 0$, (A2): $\tilde{\theta}_2(t) = 0$ and with the adaptive law for $\theta_1(t)$ (12), the state system (10) and reference system (11), the proof in Theorem 1 can be reworked to show that $\lim_{t\to\infty} e(t) = 0$.

VI. Performance Evaluation

The simulation for our adaptive control scheme is carried out using the matrices $A \in R^{4\times4}$ and $B \in R^{4\times1}$ from [4], and [10]. The states are lateral velocity $x_1(t)$, roll rate $x_2(t)$, yaw rate $x_3(t)$, roll angle $x_4(t)$. The matrices A and B are

$$A = \begin{bmatrix} -0.0134 & 48.5474 & -632.3724 & 32.0756 \\ -0.0199 & -0.1209 & 0.1628 & 0 \\ -0.0024 & -0.0526 & -0.0252 & 0 \\ 0 & 1 & 0.0768 & 0 \end{bmatrix},$$

$$B = \begin{bmatrix} 0 \\ -0.0431 \\ -0.0076 \\ 0 \end{bmatrix}.$$

The plant is open loop unstable because the poles are: $-1.2795, 0.5714 + 0.7711i, \;\; 0.5714 - 0.7711i, \; -0.0227$. Using a linear-quadratic regulator design, with input matrices A, B, Q_1 and a scalar r_1, where $Q_1 = I_4$ and $r_1 = 5$, we determine a constant gain vector

$$K = \begin{bmatrix} 0.9070 & -106.9310 & 263.3615 & -16.3616 \end{bmatrix}.$$

With this K, we have

$$A_m = \begin{bmatrix} -0.0134 & 48.5474 & -652.3724 & 32.0756 \\ 0.0192 & -4.7296 & 11.5137 & -0.7052 \\ 0.0045 & -0.8653 & 1.9763 & -0.1243 \\ 0 & 1 & 0.0768 & 0 \end{bmatrix},$$

which has closed loop poles as follows: $-1.1811, -0.7792 + 0.8684i, -0.7792 - 0.8684i,$ and -0.0272. Solving (13), using this A_m and $Q = I_4$, we get

$$P = \begin{bmatrix} P_1 & P_2 \end{bmatrix},$$

$$P_1 = \begin{bmatrix} 0.755 & 48.004 \\ 48.004 & 27930.082 \\ -314.066 & -141015.824 \\ 16.838 & 7750.340 \end{bmatrix},$$

$$P_2 = \begin{bmatrix} -314.065 & 16.838 \\ -141015.824 & 7750.340 \\ 722568.163 & -39605.211 \\ -39605.211 & 2190.417 \end{bmatrix}.$$

A. Simulation Results

For simulation, a reference signal

$$r(t) = \begin{cases} 1.5\sin(t), & 0 \leq t \leq 60 \\ 1.5\sin(t) + 3\sin(3t), & t \geq 60 \end{cases}$$

is used and under assumptions (A1) and (A2), the parameter θ_2 is assumed to be 15deg. The initial states are: lateral

velocity (0.1 ft/sec), roll rate (0.01 deg/sec), yaw rate (0.001 deg/sec) and roll angle(0.01 deg) for both types of inverses. The initial reference states are: (0.5 ft/sec), (0.1 deg/sec), (0.01 deg/sec) and (0.1 deg) respectively. An initial estimate $\theta_1(0) = 20$volts-deg for the true nonlinearity parameter $\theta_1^* = 33.33$volts-deg, lower bound of θ_1^* as $\theta_1^a = 1$volt-deg and adaptation gain $\gamma_1 = 1$ are chosen.

Simulation I. The adaptive inverse results are shown in Figures 4 - 6. Specifically, Figure 4 shows the response of state signals $x_i(t),\ i = 1, \ldots, 4$ and the reference signals $x_{mi}(t),\ i = 1, \ldots, 4$. Figure 5 shows that the tracking errors $e(t) = x_i(t) - x_{mi}(t)$ asymptotically go to zero. Figure 6 shows the input voltage and the desired state feedback control signal characteristics and also that the parameter error $\theta_1(t) - \theta_1^*$ and the control error $u(t) - u_d(t)$ asymptotically go to zero. The adaptive inverse approach does not guarantee parameter convergence and only guarantees asymptotic state tracking with parameter boundedness.

B. Effect of Saturation

In Simulation I, we tested a reference signal $r(t)$ under assumption (A1) and (A2), and obtained favorable results of adaptive inverse compensation. However, for a reference signal with a large amplitude, (A1) may fail to be true leading to the singularity of the adaptive inverse (5). In order to prevent this, we impose a restriction on $u_d(t)$ in (5). We first define the state feedback control signal

$$\bar{u}_d(t) = -Kx(t) + r(t), \tag{22}$$

choose a small $\delta > 0$, and set

$$u_d(t) = \begin{cases} \theta_2 - \delta & \text{if } \ \bar{u}_d(t) \geq \theta_2 - \delta, \text{ and} \\ \bar{u}_d(t) & \text{otherwise} \end{cases} \tag{23}$$

Simulation II. We choose $\delta = 1$ and a reference signal $\bar{r}(t) = 5r(t)$ with the control signal given by (23). The simulation results are shown in Figures 7-9. Specifically, Figure 7 and 8 show that the plant and reference states converge to each other and tracking errors go to zero respectively. Figure 9 shows the input voltage characteristics $v(t)$, the control signal characteristics $u_d(t)$, the control signal adjustment under saturation $\bar{u}_d(t) - (\theta_2 - \delta)$, and the asymptotic convergence of the parameter error $\theta_1(t) - \theta_1^*$. This particular simulation result pertaining to relaxation of assumption (A1) has not been verified by analysis.

VII. Concluding Remarks

This paper has presented a mathematical model of a synthetic jet actuator for aircraft flight control. An adaptive inverse can be derived which is capable of adaptively compensating the actuator parameter uncertainty. A state feedback control law, combined with the adaptive inverse, has been designed and analyzed which achieves desired stability and tracking performance, as demonstrated by both analysis and simulation.

Based on this result, future work for this research can be formulated. First, the input signal variables that can be manipulated for control could include the number of active jets in the array, the signal amplitude, and frequency. The control effect due to manipulation of each of these variables is a nonlinear function of these variables. Second, an increased number of actuator arrays and their position on the airfoil is another vital aspect of further work. Third, a nonlinear feedback control law is to be developed for a nonlinear aircraft dynamic model. Fourth, an analytical adaptive control framework for tracking of systems with saturation constraints is to be developed. In addition, adaptive compensation of actuator failures also needs to be incorporated so as to obtain optimal performance in the presence of unknown actuator failures.

References

[1] M. Amitay, D.R. Smith, V. Kibens, D.E. Parekh, A. Glezer, "Aerodynamic flow control over an unconventional airfoil using synthetic jet actuators," *AIAA Journal*, Vol. 39, No. 3, 361-370, 2001.

[2] M. Amitay, D. Pitt, V. Kibens, D.E. Parekh, A. Glezer, "Control of internal flow separation using synthetic jet actuators," *AIAA*, paper No. 2000-0903, 2000.

[3] M. Amitay, M. Horvath, M. Michaux, and A. Glezer, "Virtual aerodynamic shape modification at low angles of attack using synthetic jet actuators," *AIAA*, paper No. 2001-2975, 2001.

[4] S. H. Chen, G. Tao, J.T. Fei, and S.M. Joshi, "An adaptive actuator failure compensation scheme for controlling a morphing Aircraft model," *Proceedings of 42th IEEE Conference on Decision and Control,* pp 4926-4931, Maui, HI, 2003.

[5] A. Crook, N.J Wood, "Measurements and Visualizations of Synthetic Jets Actuators," *AIAA*, paper No. 2001-0145, Jan 2001.

[6] Q. Gallas, R. Holman, T. Nishida, B. Carroll, M. Sheplak, L. Cattafesta, "Lumped Element Modeling of Piezoelectric-Driven Synthetic Jet Actuators," *AIAA* paper No. 2002-125, Jan. 14-17, 2002.

[7] A. Honohan, M. Amitay, and A. Glezer, "Aerodynamic control using synthetic jets," *AIAA*, paper No. 2000-2401, 2000.

[8] F. L. Lewis, *Applied Optimal Control and Estimation*, Prentice-Hall, Englewood Cliffs, NJ, 1992.

[9] D. Lockerby, *Numerical Simulation of Boundary-Layer Control using MEMS Actuation* Ph.D Dissertation, The University of Warwick, March, 2001.

[10] D. L. Raney, R. C. Montgomery, L. L. Green and M. A. Park, "Flight Control using Distributed Shape-Change Effector Arrays," *AIAA* paper No. 2000-1560, April 3-6, 2000.

[11] W. J. Rugh, *Linear System Theory*, 2nd ed., Prentice-hall, Englewood Cliffs, NJ, 1996.

[12] D. Smith, M. Amitay, V. Kibens, D. Parekh, and A. Glezer, "Modification of the Lifting Body Aerodynamics by Synthetic Jet Actuators," *AIAA*, paper No. 98-0209, 1998.

[13] G. Tao, *Adaptive Control Design and Analysis,*, John Wiley & Sons, 2003.

[14] G. Tao and P. V. Kokotović, *Adaptive Control of Systems with Actuator and Sensor Nonlinearities,*, John Wiley & Sons, New York, 1996.

Results of Simulation I

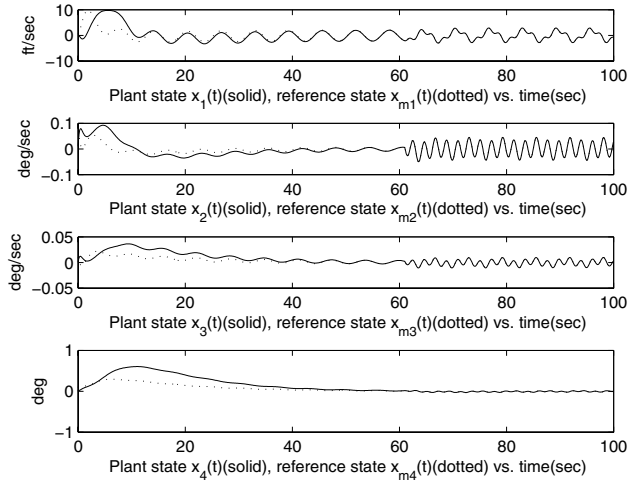

Fig. 4. Plant and reference states.

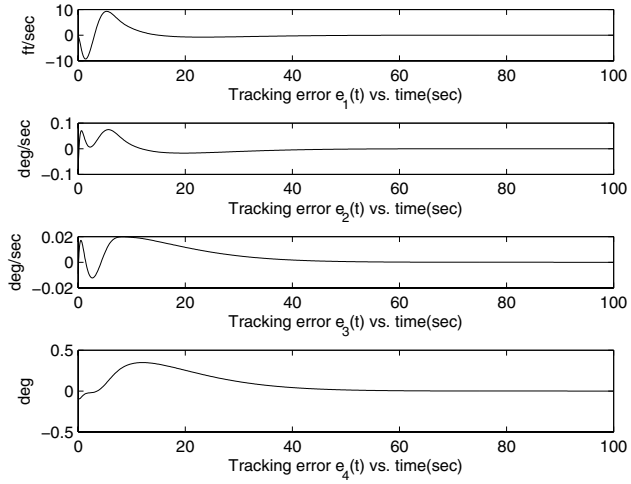

Fig. 5. State tracking errors.

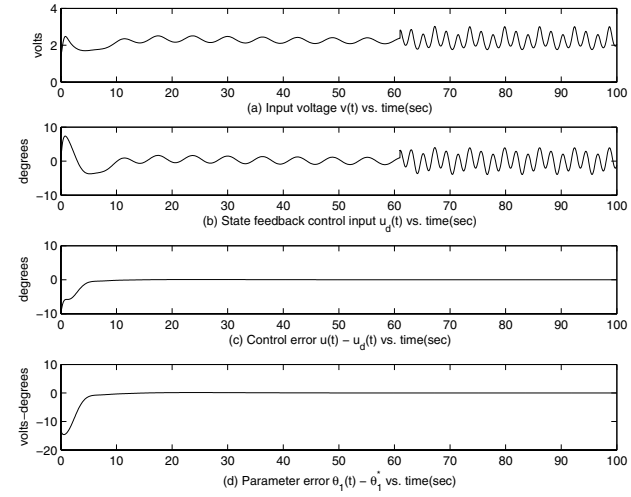

Fig. 6. (a) Input signal $v(t)$, (b) desired control signal $u_d(t)$, (c) control error $u(t) - u_d(t)$, (d) parameter error $\theta_1(t) - \theta_1^*$.

Results of Simulation II

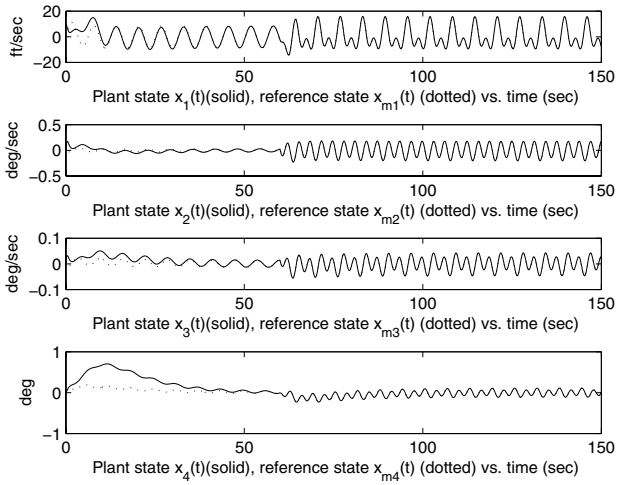

Fig. 7. Plant and reference states (under saturation).

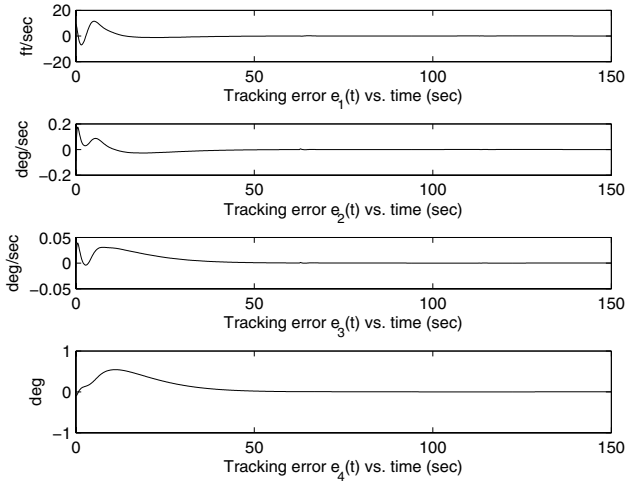

Fig. 8. State tracking errors (under saturation).

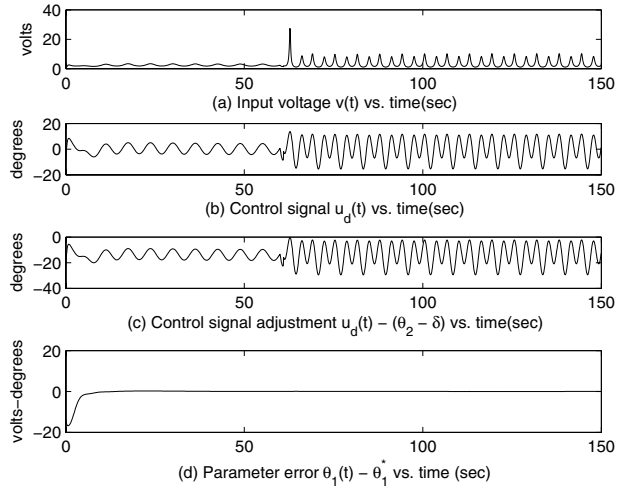

Fig. 9. (a) Input signal $v(t)$, (b) control signal $u(t)$, (c) control adjustment $\bar{u}_d(t) - (\theta_2 - \delta)$, and (d) parameter error $\theta_1 - \theta_1^*$ (under saturation).